2010

Using Spatial Uncertainty of Prior Measurements to Design Adaptive Sampling of Elevation Data

Samsuzana Abd Aziz
Universiti Putra Malaysia

Brian L. Steward
Iowa State University, bsteward@iastate.edu

Manoj Karkee
Iowa State University

Using Spatial Uncertainty of Prior Measurements to Design Adaptive Sampling of Elevation Data

Abstract
Field sampling can be a major expense for planning within-field management in precision agriculture. An efficient sampling strategy should address knowledge gaps, rather than exhaustively collect redundant data. Modification of existing schemes is possible by incorporating prior knowledge of spatial patterns within the field. In this study, spatial uncertainty of prior digital elevation model (DEM) estimates was used to locate adaptive re-survey regions in the field. An agricultural vehicle equipped with RTK-DGPS was driven across a 2.3 ha field area to measure the field elevation in a continuous fashion. A geostatistical simulation technique was used to simulate field DEMs using measurements with different pass intervals and to quantitatively assess the spatial uncertainty of the DEM estimates. The high-uncertainty regions for each DEM were classified using image segmentation methods, and an adaptive re-survey was performed on those regions. The addition of adaptive re-surveying substantially reduced the time required to resample and resulted in DEMs with lower error. For the widest sampling pass width, the RMSE of 0.46 m of the DEM produced from an initial coarse sampling survey was reduced to 0.25 m after an adaptive re-survey, which was close to that (0.22 m) of the DEM produced with an all-field re-survey. The estimated sampling time for the adaptive re-survey was less than 50% of that for all-field re-survey. These results indicate that spatial uncertainty models are useful in an adaptive sampling design to help reduce sampling cost while maintaining the accuracy of the measurements. The method is general and thus not limited to elevation data but can be extended to other spatially variable field data.

Keywords
Adaptive sampling, Digital elevation model, Sequential Gaussian simulation, Spatial uncertainty

Disciplines
Agriculture | Bioresource and Agricultural Engineering

Comments
This article is from *Transactions of the ASABE*, 53, no. 2 (2010): 349–357.

USING SPATIAL UNCERTAINTY OF PRIOR MEASUREMENTS TO DESIGN ADAPTIVE SAMPLING OF ELEVATION DATA

S. Abd Aziz, B. L. Steward, M. Karkee

ABSTRACT. *Field sampling can be a major expense for planning within-field management in precision agriculture. An efficient sampling strategy should address knowledge gaps, rather than exhaustively collect redundant data. Modification of existing schemes is possible by incorporating prior knowledge of spatial patterns within the field. In this study, spatial uncertainty of prior digital elevation model (DEM) estimates was used to locate adaptive re-survey regions in the field. An agricultural vehicle equipped with RTK-DGPS was driven across a 2.3 ha field area to measure the field elevation in a continuous fashion. A geostatistical simulation technique was used to simulate field DEMs using measurements with different pass intervals and to quantitatively assess the spatial uncertainty of the DEM estimates. The high-uncertainty regions for each DEM were classified using image segmentation methods, and an adaptive re-survey was performed on those regions. The addition of adaptive re-surveying substantially reduced the time required to resample and resulted in DEMs with lower error. For the widest sampling pass width, the RMSE of 0.46 m of the DEM produced from an initial coarse sampling survey was reduced to 0.25 m after an adaptive re-survey, which was close to that (0.22 m) of the DEM produced with an all-field re-survey. The estimated sampling time for the adaptive re-survey was less than 50% of that for all-field re-survey. These results indicate that spatial uncertainty models are useful in an adaptive sampling design to help reduce sampling cost while maintaining the accuracy of the measurements. The method is general and thus not limited to elevation data but can be extended to other spatially variable field data.*

Keywords. *Adaptive sampling, Digital elevation model, Sequential Gaussian simulation, Spatial uncertainty.*

Precision agriculture is a farming system that aims to improve crop yield and quality while reducing input cost and minimizing environmental impact. An important key to efficient and effective precision agriculture is to match resource inputs to the spatial and temporal variability of field attributes through site-specific management. In the past, managers used field-scale estimates and treated farm fields uniformly as single units. Site-specific management, however, requires an understanding of spatial variability within the field, and hence sampling is needed to estimate attributes at a smaller scales than whole-field scale.

Field sampling can be a major expense for planning within-field management in precision agriculture. Locating the samples inappropriately or taking more samples than are needed can result in extra expense. Taking too few samples, on the other hand, may not accurately characterize in-field variability. Conventionally, grid sampling was used in gathering field attributes. Sample points were located at the nodes or centers of square, rectangular, or other regular-shaped grids on the field, where the locations can be established and maintained using GPS. Gridded schemes are convenient to locate and analyze but, like traditional simple random sampling schemes, may be inefficient to precisely capture the spatial variability of the attributes and somewhat ignore actual local variability.

Recently, continuous vehicle-based sampling has been investigated due to proliferation of automatic guidance systems on agricultural vehicles with high-accuracy GPS capability and advanced sensor technology. Such sampling requires less labor and offers a rapid and relatively easy way for producers to obtain field data. Examples include vehicle-mounted GPS systems to collect elevation data (Clark and Lee, 1998; Westphalen et al., 2004; Schmidt et al., 2003), continuous soil sampling systems to sample soil attributes on-the-go (Saito et al., 2008), and electrical conductivity (EC) mobile sensors to measure soil EC continuously in the field (Corwin and Lesch, 2005; Sudduth et al., 2001). Vehicle-based sampling is characterized by highly dense data along the travel pass and no samples between the passes. Again, like grid sampling, the question comes back to where exactly to sample to efficiently capture the variability in the field.

An efficient sampling strategy should address knowledge gaps rather than exhaustively collect redundant data. Hence, a "smart sampling" plan should be conducted for efficient data collection and improved estimates of the variability. Modification of existing schemes is possible by incorporating prior knowledge of spatial variability within the

Submitted for review in July 2009 as manuscript number PM 8110; approved for publication by the Power & Machinery Division of ASABE in March 2010. Presented at the 2008 ASABE Annual Meeting as Paper No. 084826.

The authors are **Samsuzana Abd Aziz, ASABE Member Engineer,** Senior Lecturer, Department of Biological and Agricultural Engineering, Faculty of Engineering, Universiti Putra Malaysia, Selangor, Malaysia; **Brian L. Sterward, ASABE Member Engineer,** Associate Professor, and **Manoj Karkee, ASABE Member Engineer,** Assistant Scientist, Department of Agricultural and Biosystems Engineering, Iowa State University, Ames, Iowa. **Corresponding author:** Samsuzana Abd Aziz, Department of Biological and Agricultural Engineering, Faculty of Engineering, Universiti Putra Malaysia, 43400 UPM Serdang, Selangor DE, Malaysia; phone: +603-8946-4326; fax: +603-8946-6425; e-mail: suzana@eng.upm.edu.my.

  ISSN 2151-0032

field. Field elevation in the form of digital elevation models (DEMs) is among the most important attributes that can provide information about the spatial variability in the field (Kravchenko and Bullock, 2000; Kaspar et al., 2003; Rampant and Abuzar, 2004; Jiang and Thelen, 2004). This article reports on research to investigate a method to efficiently implement vehicle-based sampling to collect elevation data in farm fields.

Many studies have sought to quantify DEM accuracy and compare the accuracy of DEMs produced using different data sources and production methods. By comparing with higher-grade measurement data sources, measures such as standard deviation or root mean square error (RMSE) are typically used to represent the DEM quality. Such non-spatial statistics are global measures and specifically do not provide an assessment of how accurately each grid in a DEM represents a true elevation (Wise, 1998; Wechsler, 2007).

Moreover, survey-grade measurements are costly to obtain, and in some locations, impractical to obtain. Due to this limitation, researchers have investigated other ways to assess local quality of DEMs. A number of authors recognized that spatial simulation methods can be used for uncertainty assessment of DEM quality (Hunter et al., 1995; Holmes et al., 2000; Carlisle, 2005; Wechsler and Kroll, 2006). The simulation process accounts for spatial correlation in the data to produce multiple estimates (realizations) for each particular location in the DEM. These realizations provide a range within which the true estimate lies (Wechsler, 2007). The variance of the elevation realizations for each DEM grid can be used as an uncertainty measure of the estimate in the grid. The advantage of using this technique is that it preserves the nature of real-world variability and spatial correlation in the estimates without the smoothing of the interpolated estimates, which usually occurs in kriging (Goovaerts, 1997).

In the research described in this article, sequential Gaussian simulation (SGS) was used to estimate spatial uncertainty of elevation data for designing a sampling strategy. Among many other conditional simulations techniques, SGS is by far the most widely used to estimate continuous variables like elevation (Journel and Huijbregts, 1978). Detailed descriptions of the SGS method can be found in Goovaerts (1997). The SGS method used in this study was selected because of its simplicity and efficiency, not because of any perceived theoretical superiority. Sequential indicator simulation (SIS) (Deutsch and Journel, 1998) might deal more easily with the data, but it is relatively cumbersome to use. Other conditional simulation algorithms, such as turning bands (Journel, 1974), Monte Carlo (Heuvelink et al., 1989), simulated annealing (Deutsch and Journel, 1998), and random fields (Wechsler and Kroll, 2006), could be expected to produce similar results. For example, Kravchenko (2003) used a simulated annealing procedure to simulate data sets with different spatial structure based on soil sample data to evaluate the effect of data variability and strength of spatial correlation in the data on performance of grid soil sampling and interpolation procedures. She found that the accuracy achieved in mapping soil properties strongly depended on spatial structure: the stronger the spatial correlation, the more accurate the soil property map. Hence, information about spatial structure of the data is important for mapping soil properties.

In this study, the spatial uncertainty of elevation estimates from a preliminary field sampling survey were used as a rational basis for designing adaptive resampling surveys to improve the accuracy of field DEMs. The uncertainty of elevation estimates across the DEMs was assessed using a geostatistical simulation technique to delineate the regions in the field that needed to be resampled. Additional samples could then be targeted and obtained from specified locations rather than re-surveying the entire field. The goal of this study is to develop a method for designing adaptive resampling field surveys based on spatial uncertainty from an initial field survey. Specific objectives included:

- Determining the improvement in DEM accuracy with adaptive re-surveys as compared to that obtained with all-field re-surveys.
- Understanding the interaction between initial sampling coarseness and data variability in DEM uncertainty.
- Estimating the reduction in sampling time for adaptive re-surveys as compared with all-field re-surveys.

METHODS

FIELD STUDY AND DATA PREPARATION

Data were collected from a portion of a 6.5 ha (16 acre) field that had been chisel-plowed after the previous corn crop had been harvested. Elevation data were collected using a self-propelled agricultural sprayer (model 4710, Deere & Co., Moline, Ill.) equipped with a real-time kinematic differential GPS (RTK-DGPS) receiver (StarFire RTK, Deere & Co., Moline, Ill.) operating at 1 Hz. The RTK-DGPS has a vertical static RMSE of less than 1.5 cm plus an additional 1 ppm of the distance to the base station. This additional error was less than 0.04 cm because the maximum distance to the base station was about 350 m (1150 ft). The GPS receiver was mounted at a height of 3.81 m above the field surface. The vehicle was driven over a 2.3 ha (5.7 acre; 247.55 m wide × 294.96 m long) area of the field at a speed between 6.4 to 9.7 km h^{-1} (4 to 6 mph) along northwest-southeast passes in a headland pattern with opposite travel directions on adjacent measurement passes (Westphalen et al., 2004). The passes were 3.05 m (10 ft) apart. Further details about this elevation data collection methodology and associated error analysis can be found in Westphalen et al. (2004) and Abd Aziz et al. (2009).

Since the raw data were in the format of a geographic coordinate system consisting of longitude, latitude, and altitude, the data were projected so that spatial data analysis preceded using units of length in the horizontal plane. The standard USGS Universal Transverse Mercator (UTM) projection was used (UTM grid zone 15N) for the coordinate projection with all units for easting, northing, and elevation in meters.

Every other measurement along the measurement passes was subsampled and used as the calibration group. The remaining measurements were used as the validation group to measure the quality of the simulated elevation. To simulate the effect of driving the vehicle at measurement passes greater than 3.05 m apart, the calibration data group was jackknifed into seven separate subgroups by skipping data along passes at a regular interval. These subgroups corresponded to intervals of 6.10 m, 9.15 m, 12.20 m, 15.25 m, 18.30 m, 21.35 m, and 24.40 m between passes.

These seven datasets became the initial sampling data from which the field DEMs were simulated to assess the uncertainty in the elevation estimates.

Conditional Simulation

The spatial uncertainty of the elevation was modeled using the SGS method performed with the gstat program in R statistical software (Free Software Foundation, Inc., Boston, Mass.). A grid size of 1 m was chosen as a trade-off between sufficient resolution and required computation time. Prior to the simulation process, the normal scores transform, a non-linear transform that remaps any distribution to a normal distribution (Goovaerts, 1997), was applied to the datasets to map the data distribution into a standard normal distribution. This was done to meet the format requirement of Gaussian simulation, that the univariate distribution of the data be standard normal. The sample variogram of the normal score transformed data was then fit with a linear variogram model with a 20 m lag distance and zero nugget effect. A linear variogram model was used because the semivariances did not reach a sill. This was due to the fact that elevation data have the potential to become more and more variable over larger distances due to surficial processes (Holmes et al., 2000).

In the SGS routine, simple kriging was performed to find an elevation estimate and standard deviation used for the Gaussian conditional cumulative distribution function (ccdf). The elevation estimate from simple kriging was based on the normal score data and values simulated at previously visited grids. From the ccdf, a value was then selected at random and added to the data set. The search radius of the kriging estimator was set to the range of the variogram and a minimum of 16 data points. A total of 100 simulations were run, resulting in 100 realizations in each DEM grid. The mean of these realizations in each grid was calculated to produce the mean estimate, which is also known as the E-type estimate of the grid. The E-type estimate across the DEM was used to produce the map of DEM estimates. The variance of the realizations, also known as the conditional variance, was used to quantify the uncertainty of the DEM estimates. SGS was applied individually to the seven subgroups with different measurement pass distances.

Adaptive Sampling

The conditional grid variance from the simulation process was used as the uncertainty estimate of the DEM. Conditional variance maps were then used to characterize the regions that needed to be resampled. Using an estimation variance threshold of 0.04 m^2, the field was classified into regions of high and low estimation uncertainty. This threshold value was chosen because the variance histogram showed a distinct separation at 0.04 m^2. After initial grid classification, morphological operations were applied to filter out segmentation noise and scattered unconnected pixels. Scattered unconnected pixels may correspond to random noise introduced from SGS and should not be considered a valid region of interest. The Matlab (The Mathworks, Natick, Mass.) morphological operations function bwmorph was used to perform a "cleaning" operation, followed by "filling" and "removing" operations to remove the noise. After filtering, the resulting areas of high uncertainty were chosen for an adaptive resampling survey.

In the application of an adaptive resampling survey, new samples should only be acquired in the regions of interest. Hence, for the experimental design of the study, unused measurement passes that fell in the regions that exceeded the estimation variance threshold were added to each initial sampling subgroup. Only one unused measurement pass in between initial measurement passes in the delineated region was used to uniformly simulate the effect of adding newly adaptive resampled data within the division of data subgroups (fig. 1). SGS was then performed on the new sampling sets to produce improved DEM estimates, as well as their associated uncertainty.

For comparison, an all-field resampling survey was simulated by adding full unused measurement passes between initial measurement passes across the whole study area. Again, only one unused measurement pass in between initial measurement passes was used to uniformly simulate the effect of adding new all-field re-survey data within the division of data subgroups.

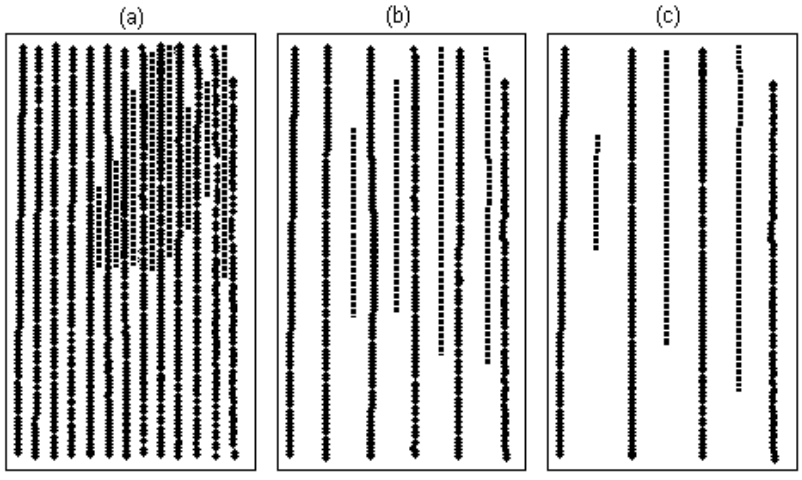

Figure 1. Measurements passes at (a) 6.10 m, (b) 15.25 m, and (c) 24.40 m intervals (diamonds) with additional adaptive re-survey measurements between the passes (squares).

Data Analysis

Sampling Time

The amount of time spent to collect data within each subgroup for adaptive re-surveys and all-field re-surveys was estimated based on the travel distance and the vehicle speed used for traveling along the passes as well as making turns. Since the vehicle velocity was in the range of 6.4 to 9.7 km h^{-1} (4 to 6 mph) during the survey, the minimum speed, 6.4 km h^{-1} (4 mph), was used to estimate the travel time. The vehicle velocity while making turns between passes was slower and was estimated to be around 3.2 km h^{-1} (2 mph).

DEM Error Estimation

A total of 21 DEMs were developed from the calibration subgroups. These DEMs were compared to the validation dataset from the validation group, which had not been used to simulate the elevation surface. RMSE, the typical measure of DEM error (Wise, 1998), was calculated by subtracting the elevation of the nearest estimated point from that of each validation point. The DEMs produced from the initial sampling survey were used as the controls to evaluate the effect of adding new adaptive and non-adaptive sample data in mapping the field elevation.

Slope Estimation

One of the common needs in quantitative DEM interpretation is to determine terrain slope, which is the rate of elevation change in the direction of the steepest descent. Terrain slope is frequently used to determine water flow direction in hydraulic analysis or surface erosion and environmental impact in agricultural and environmental studies. To study the effects of sampling procedures on slope prediction, the slope derivatives from each generated DEM were calculated using ArcGIS (version 9.2, ESRI, Redlands, Cal.). The DEMs were imported into ArcGIS, and a slope calculation extension was used in the ArcMap Spatial Analyst to automatically calculate the slope. The accuracy of the slope was quantified by comparing the estimated value with the slope derived from the DEM developed using the validation data. The RMSE was calculated by subtracting the estimated slope in each grid from the slope value in the corresponding grid of the validation DEM.

Slope Uncertainty

Calculation of slope in ArcGIS is based on the first partial derivatives of elevation, z (Burrough and McDonell, 1998):

$$p = \frac{\partial z}{\partial x} \tag{1}$$

$$q = \frac{\partial z}{\partial y} \tag{2}$$

where p is the change of height in the directions of the x-axis (easting), and q is the change of height in the direction of the y-axis (northing). The values of the partial derivatives were approximated in 3×3 grid neighborhoods using equations 3 and 4. The top row of the 3×3 neighborhood elevations are represented by z_1, z_2, z_3; the middle row by z_4, z_5, z_6; and the bottom row by z_7, z_8, z_9. The distance between adjacent points or the grid size is denoted by w:

$$p \approx \frac{(z_3 + 2z_6 + z_9) - (z_1 + 2z_4 + z_7)}{8w} \tag{3}$$

$$q \approx \frac{(z_7 + 2z_8 + z_9) - (z_1 + 2z_2 + z_3)}{8w} \tag{4}$$

The slope (S) of a grid was calculated using equation 5:

$$S = \sqrt{p^2 + q^2} \tag{5}$$

Based on this formulation, the uncertainty in the slope estimates (ΔS) was calculated using the sensitivity coefficients with respect to the nine neighboring estimates (z_i), each with their own uncertainty (Δz_i, obtained from the conditional simulation method):

$$\Delta S = \sqrt{\left(\frac{\partial S}{\partial p}\right)^2 (\Delta p)^2 + \left(\frac{\partial S}{\partial q}\right)^2 (\Delta q)^2} \tag{6}$$

where

$$\Delta p = \sqrt{\sum \left(\frac{\partial p}{\partial z_i}\right)^2 (\Delta z_i)^2} \tag{7}$$

$$\Delta q = \sqrt{\sum \left(\frac{\partial q}{\partial z_i}\right)^2 (\Delta z_i)^2} \tag{8}$$

The uncertainty of the derived slope for each DEM was visually assessed using a contour plot of the mean elevation and the variance.

Results and Discussions

Conditional Variance Maps

The conditional variance maps produced using SGS reveal clear correlation of the uncertainties in DEM with the slope of the land surface (fig. 2). Based on the measured data, conditional variance is larger in the steepest area (northeast) of the field, where elevation values change the most. The variance values ranged from 0.10 to 0.16 m^2 in this area. The uncertainty is small in the south and northwest of the study area, where the terrain has less slope. The variance ranged from 0 to 0.04 m^2 in this area.

Histograms of the grid variance in the conditional variance maps were plotted by measurement subgroup to verify the appropriateness of the chosen threshold value (fig. 3). The histograms had a strong multimodality because

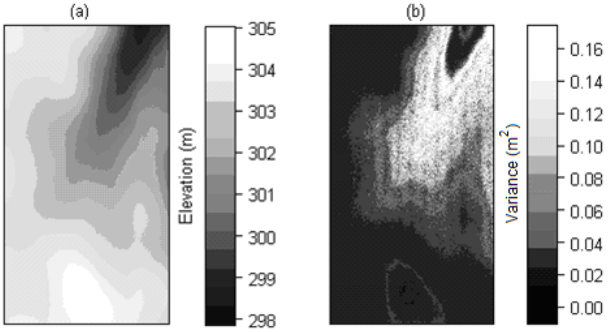

Figure 2. (a) Mean elevation (E-type) estimate and (b) corresponding conditional variance map of the DEM generated from SGS using measurements with 6.10 m pass intervals.

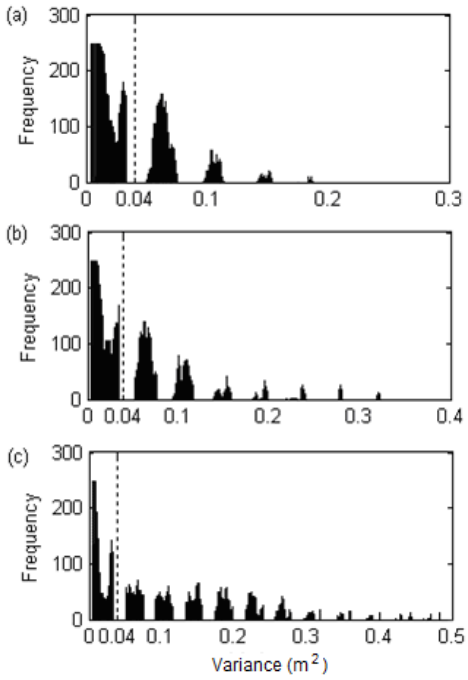

Figure 3. Histograms of SGS variance estimates using measurement passes at (a) 6.10 m, (b) 15.25 m, and (c) 24.40 m intervals. The dashed vertical line is the variance threshold above which grids were classified as highly uncertain regions.

the simulation process relies not only on the variability of the elevation values but also on the distance to the sampling measurements. The measurements were collected systematically along parallel passes, and the simulation process captured this sampling pattern. In all cases, the mode with the highest frequency had values ranging from 0 to 0.04 m^2 and was clearly separated from the other modes. This distribution corresponded to grids that have little change in elevation and were situated closer to sampling measurements. The subgroup with 6.10 m measurement intervals has a variance distribution with the smallest range, from 0 to 0.19 m^2, relative to other measurement subgroups. As the measurement interval increased, the variance distribution spread to larger ranges. Thus, the 0.04 m^2 variance threshold was adequate to classify the variance estimates into high and low uncertainty classes.

Adaptive Resampling Analysis

Based on the conditional variance maps and the variance threshold, low-uncertainty regions were those with conditional variance below the threshold (shown as black; fig. 4), and high-uncertainty regions had conditional variance above the threshold (shown as white; fig. 4). As expected, sparser sampling led to more uncertainty in the estimated values. Visually, the DEM developed using measurements with a pass interval of 24.4 m had the largest high-uncertainty region of about 57% of the total area (fig. 4c). The high-uncertainty region for the DEM developed using measurements with passes interval of 6.10 m was smaller (around 18%) and located at the region where elevation values changed the most (fig. 4a). In this case, the SGS captured the actual elevation variability.

The size of the high-uncertainty regions decreased as the interval width of the measurements passes used in data

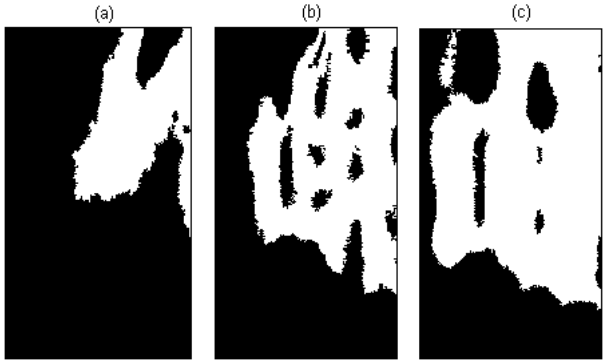

Figure 4. Conditional variance maps for measurements at (a) 6.10 m, (b) 15.25 m, and (c) 24.40 m pass intervals were transformed into binary images. Low-uncertainty regions (white) were classified by image segmentation with the 0.4 m^2 threshold followed by the morphological operation functions of "cleaning," "filling," and "removing" implemented in Matlab.

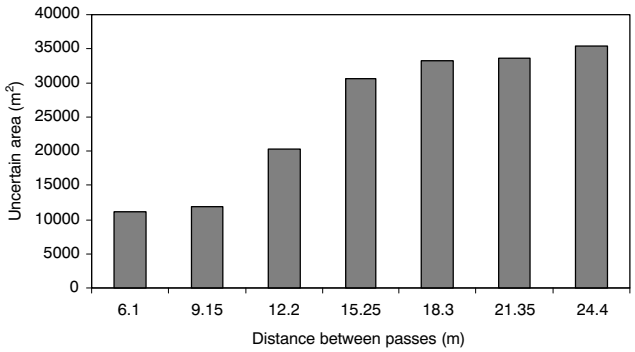

Figure 5. Area classified as highly uncertain based on conditional variance of DEMs increased with distance between measurement passes.

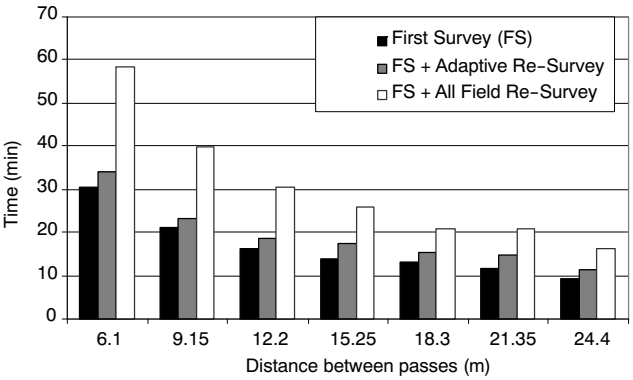

Figure 6. Estimated time to collect the elevation data with additional adaptive and all-field re-survey measurements as a function of distance between passes.

Table 1. Area classified as highly uncertain by measurement interval subgroup.

Interval Subgroup	No. of Passes Skipped	No. of Passes Used[a]	No. of Data Points	Area Classified as Highly Uncertain (m^2)
6.10 m	1	13	1142	11229
9.15 m	2	9	793	11963
12.20 m	3	6	541	20381
15.25 m	4	6	523	30593
18.3 m	5	5	428	33259
21.35 m	6	4	441	33667
24.4 m	7	3	356	35432

[a] Number of measurement passes used for analysis.

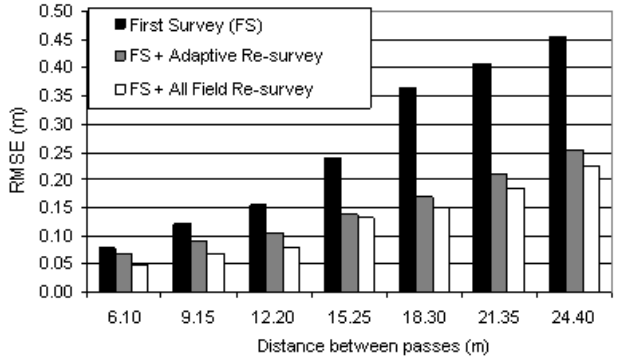

Figure 7. RMSE of DEMs developed using measurements across different passes intervals and with additional adaptive and all-field re-survey measurements between the passes.

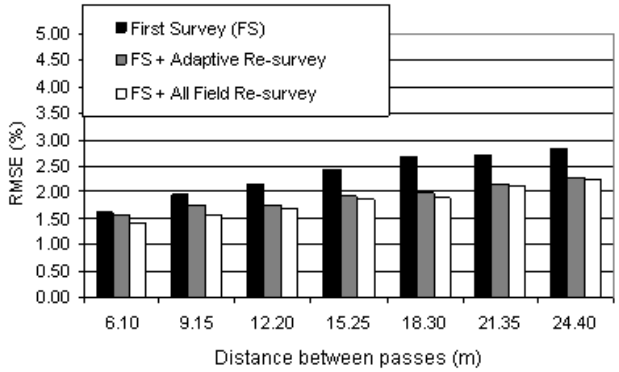

Figure 8. RMSE of slope derived from DEMs developed using measurements across different passes interval and with additional adaptive and all-field re-survey measurements between the passes.

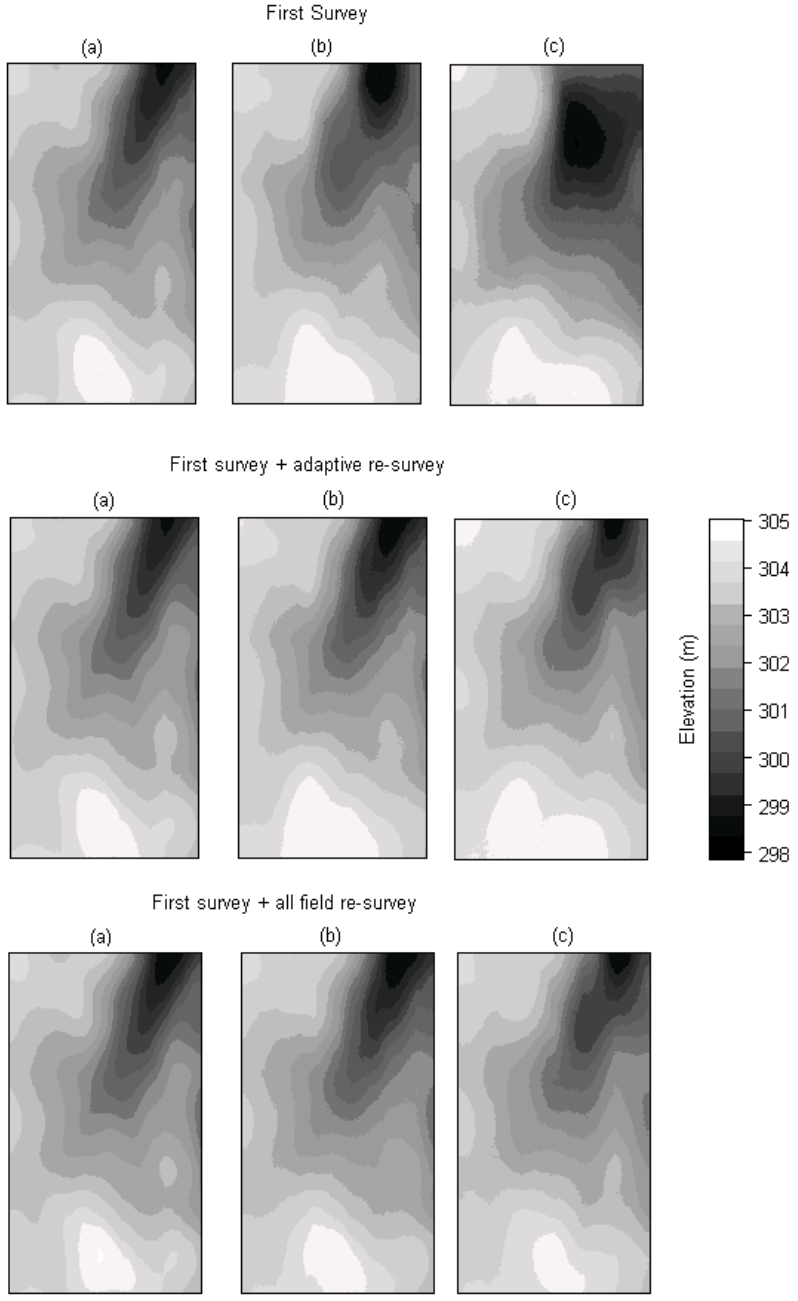

Figure 9. Contour plots of DEMs using measurements at (a) 6.10 m, (b) 15.25 m, and (c) 24.40 m pass intervals.

sampling decreased (fig. 5). This result showed that, in addition to elevation variability, the uncertainty also depends on the distance between the estimates and the sampling locations. For this study field, the sampling measurements with interval widths less than 10 m adequately captured the spatial variability in the elevation and have uncertain regions of about 11,200 m^2. Although the number of measurement passes for the 9.15 m subgroup was substantially lower than for the 6.10 m subgroup, the area of the high-uncertainty region was about the same for both interval subgroups (table 1). This result shows that, given this information, one might want to sample at a 9.15 m interval rather than a 6.10 m interval because both would capture similar variability of the field. With interval widths larger than 10 m, the high-uncertainty regions ranged from 20,300 to 35,400 m^2. The large increase in uncertainty region area between 9.15 m and 15.25 m in the graph was due to the effect of skipping measurement passes. Skipping three or more measurement passes resulted in substantially fewer measurement passes for analysis (table 1).

The collection time for adaptive re-surveys and all-field re-surveys was estimated across measurement subgroups. For both cases, the estimated time decreased as the distance between passes increased (fig. 6). The estimated time ranged from around 16 to 60 min for all-field re-surveys and around 11 to 35 min for adaptive re-surveys. Adaptive re-surveying substantially reduced the time for resampling, which is important in minimizing the cost of acquiring data.

Error Analysis

The RMSE increased as the distance between passes increased for DEMs across measurement subgroups and with adaptive and all-field re-survey measurements between the passes (fig. 7). Adaptive and all-field re-surveys reduced the RMSE of the DEMs developed using the initial sampling surveys. For the smallest sampling pass interval of 6.10 m, the RMSE of the DEM was 0.08 m and decreased to 0.07 and 0.05 m with adaptive and all-field re-surveys, respectively. For the widest measurement interval of 24.40 m, the RMSE of the DEM was 0.45 m and decreased to 0.25 and 0.22 m with adaptive and all-field re-surveys, respectively. Although the RMSEs of the DEM developed with adaptive re-surveys were slightly higher than those with all-field re-surveys, the estimated time spent for adaptive surveys was substantially lower than that of all-field re-surveys. For the sample pass distance of 15.25 m, the RMSEs of DEMs with adaptive and all-field re-surveying were not much different from each other (0.14 and 0.13 m, respectively). However, the estimated sampling time for adaptive re-surveying was more than 50% lower than that of all-field re-surveying. The adaptive re-survey method could help reduce the data collection time, which may result in lower cost while maintaining the accuracy of the measurements.

The RMSE of the slope estimates increased as the interval distance between measurement passes increased (fig. 8). Additional measurements slightly improved the slope

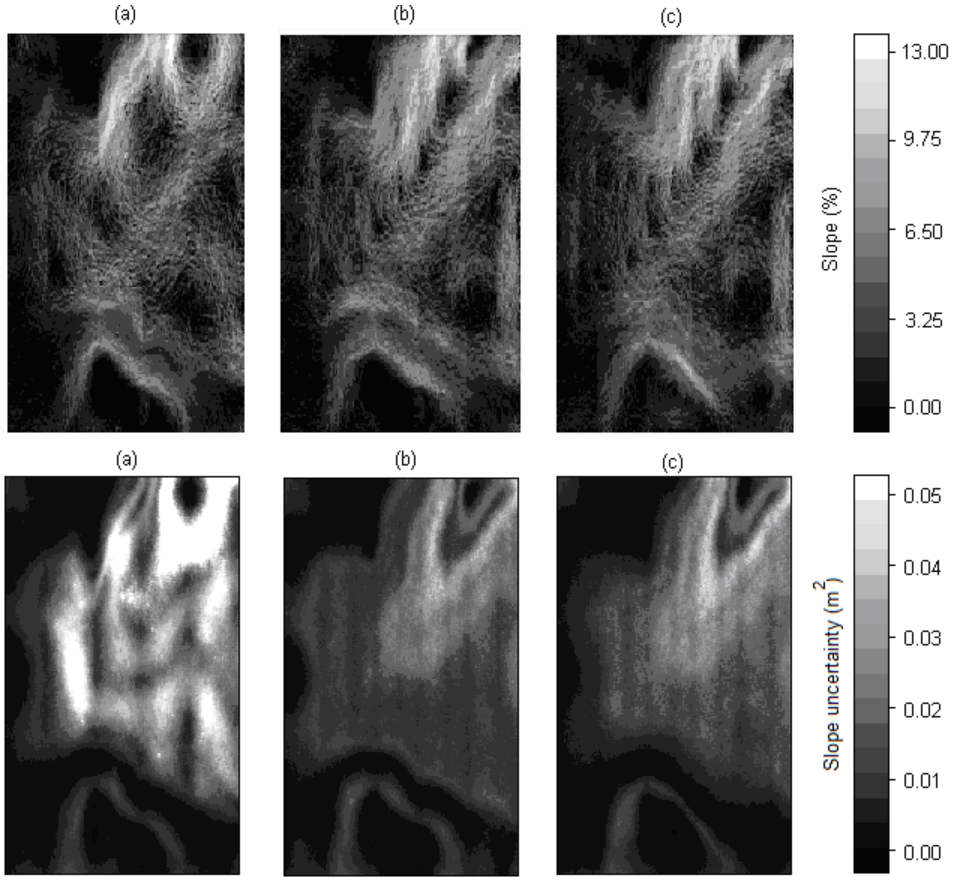

Figure 10. (a) Plots of slope using measurements at 15.25 m pass intervals (top) and associated uncertainty maps (bottom). Additional adaptive and all-field re-survey measurements were added to generate maps in (b) and (c), respectively.

estimation for smaller measurement intervals, and more significant improvement was observed for larger measurement intervals. For the smallest measurement interval of 6.10 m, the RMSE of the slope derived from the DEM was 1.6% and decreased to 1.5% and 1.4% with additional adaptive and non-adaptive measurements, respectively. For the widest measurement interval of 24.4 m, the RMSE of the slope derived from the DEM was 2.8% and decreased to about 2.2% with additional adaptive or all-field re-survey measurements. The difference in slope RMSE between DEMs with additional adaptive and all-field re-survey measurements was very small; hence, the adaptive re-survey, which requires less time for data collection, is preferable.

Generally, the re-surveying led to better estimation of the elevation and slope estimates. The quantitative results were confirmed by visual inspection of contour plots generated from the DEMs at different passes intervals (fig. 9). The addition of measurements either through the adaptive or all-field re-survey led to higher spatial frequency content in the contour lines. For the DEMs developed using a 24.4 m measurement pass interval, the sparcity of data led to substantial distortion in the DEM interpolated from the first sampling. The distortion was reduced with the addition of measurements either through adaptive or all-field re-surveys.

The calculated slope ranged from 0% to about 13% (fig. 10). The maps of the slope show a clear pattern of surface changes related to the DEMs. The pattern of slope changes was visibly more related to the DEM as the additional adaptive or all-field re-survey measurements were added. The estimated uncertainty of the slope derivation exhibits a pattern similar to the estimated conditional variance of the DEM. For 15.5 m measurement pass intervals, the slope uncertainty ranged around 0.05%. The addition of measurement passes, either through adaptive or all-field re-surveys, substantially reduced the uncertainty of the derived slope (fig. 10). The information about uncertainty in the slope derivatives may be useful to study error propagation in subsequent applications.

CONCLUSIONS

SGS was used to simulate field DEMs using measurements with different pass intervals and to quantitatively assess the spatial uncertainty of the DEM estimates. The high-uncertainty regions for each DEM were classified using image segmentation methods, and adaptive re-surveying was performed on those regions. The addition of adaptive re-survey measurements substantially reduced the time required to resample and resulted in DEMs with lower error. From this study, the following conclusions can be drawn:

- The addition of adaptive re-survey measurements resulted in DEMs with relatively lower error. For the widest sampling pass width, the RMSE of 0.46 m of the DEM produced from an initial coarse sampling survey was reduced to 0.25 m after an adaptive re-survey, which was close to that (0.22 m) of the DEM produced with an all-field re-survey.
- Uncertainty assessment using SGS quantified the variability of attributes in the field based on available sampled data. The size of the high-uncertainty regions was affected by the initial sampling coarseness as well as the actual variability in the elevation. The high-uncertainty regions were located at regions where elevation values changed the most and decreased as the interval width of the measurement passes used in data sampling decreased. The information about uncertainty is useful to study error propagation in spatial attribute estimation processes.
- The estimated sampling time for adaptive re-surveying was less than 50% of that for all-field re-survey. Use of adaptive re-surveying may efficiently aid field attribute estimation for site-specific management practices. The method could help reduce data collection time, which may result in lower cost while maintaining the accuracy of the measurements.

REFERENCES

Abd Aziz, S., B. L. Steward, L. Tang, and M. Karkee. 2009. Utilizing repeated GPS surveys from field operations for development of agricultural field DEMs. *Trans ASABE* 52(4): 1057-1067.

Burrough, P. A., and R. McDonnell. 1998. *Principles of Geographical Information Systems.* New York, N.Y.: Oxford University Press.

Carlisle, B. H. 2005. Modelling the spatial distribution of DEM error. *Trans. in GIS* 9(4): 521-540.

Clark, R. L., and R. Lee. 1998. Development of topographic maps for precision farming with kinematic GPS. *Trans. ASAE* 41(4): 909-916.

Corwin, D. L., and S. M. Lesch. 2005. Apparent soil electrical conductivity measurements in agriculture. *Computers and Electronics in Agric.* 46: 11-43.

Deutsch, V. D., and A. G. Journel. 1998. *GSLIB Geostatistical Software Library and User's Guide.* London, U.K.: Oxford University Press.

Goovaerts, P. 1997. *Geostatistics for Natural Resources Evaluation.* New York, N.Y.: Oxford University Press.

Holmes, K. W., O. A. Chadwick, and P. C. Kyriakidis. 2000. Error in a USGS 30-meter digital elevation model and its impact on terrain modeling. *J. Hydrol.* 233: 154-173.

Heuvelink, G., P. Burrough, and A. Stein. 1989. Propagation of errors in spatial modeling with GIS. *Intl. J. Geographical Info. Systems* 3(4): 303-322.

Hunter, G. J., M. Caetano, and M. F. Goodchild. 1995. A methodology for reporting uncertainty in spatial database products. *Urban and Regional Information Systems Assoc. J.* 7(2): 11-21.

Jiang, P., and K. D. Thelen, 2004. Effect of soil and topographic properties on crop yield in a north-central corn-soybean cropping system. *Agron. J.* 96(1): 252-258.

Journel, A. G. 1974. Geostatistics for conditional simulation of ore bodies. *Economic Geology* 69(5): 673-687.

Journel, A. G., and C. J. Huijbregts. 1978. *Mining Geostatistics.* New York, N.Y.: Academic Press.

Kaspar, T. C., T. S. Colvin, D. B. Jaynes, D. L. Karlen, D. E. James, D. W. Meek, D. Pulido, and H. Butler. 2003. Relationship between six years of corn yields and terrain attributes. *Precision Agric.* 4(1): 87-101.

Kravchenko, A. N. 2003. Influence of spatial structure on accuracy of interpolation methods. *SSSA J.* 67(5): 1564-1571.

Kravchenko, A. N., and D. G. Bullock. 2000. Correlation of corn and soybean grain yield with topography and soil properties. *Agron. J.* 92(1): 75-83.

Rampant, P., and M. Abuzar. 2004. Geophysical tools and digital elevation models: Tools for understanding crop yield and soil variability. In *Supersoil 2004: Proc. 3rd Australian New*

Zealand Soils Conf. Available at: www.regional.org.au/au/asssi/. Accessed 9 March 2007.

Saito, M., T. Kataoka, H. Okamoto, and S. Hata. 2008. Development of automatic continuous soil sampling system. *J. Japanese Soc. Agric. Machinery* 70(4): 123-128.

Schmidt, J. P., R. K. Taylor, and R. J. Gehl. 2003. Developing topographic maps using a sub-meter accuracy global positioning receiver. *Applied Eng. in Agric*. 19(3): 291-300.

Sudduth, K. A., S. T. Drummond, and N. R. Kitchen. 2001. Accuracy issues in electromagnetic induction sensing of soil electrical conductivity for precision agriculture. *Computers and Electronics in Agric.* 31(3): 239-264.

Wechsler, S. P. 2007. Uncertainties associated with digital elevation models for hydrologic applications: A review. *Hydrol. Earth Syst. Sci*. 11(4): 1481-1500.

Wechsler, S. P., and C. N. Kroll. 2006. Quantifying DEM uncertainty and its effect on topographic parameters. *Photogram. Eng. and Remote Sensing* 72(9): 1081-1090.

Westphalen, M. L., B. L. Steward, and S. Han. 2004. Topographic mapping through measurement of vehicle attitude and elevation. *Trans. ASAE* 47(5): 1841-1849.

Wise, S. M. 1998. The effect of GIS interpolation errors on the use of digital elevation models in geomorphology. In *Landform Modelling and Analysis*, 139-164. S. N. Lane, K. S. Richards, and J. H. Chandler, eds. Chichester, U.K.: John Wiley and Sons.